Proceedings of ASME Turbo Expo 2003
Power for Land, Sea, and Air
June 16–19, 2003, Atlanta, Georgia, USA

GT2003-38796

INVESTIGATION OF NUMERICAL AND PHYSICAL MODELLING EFFECTS ON THE CFD SIMULATION OF THE UNSTEADY FLOW IN AN HPT STAGE

P. de la Calzada
Aerodynamics and Systems Department
ITP, Industria de Turbo Propulsores S.A. Madrid, Spain
pedro.delacalzada@itp.es

J. Fernández-Castañeda
Technology and Methods Department
ITP, Industria de Turbo Propulsores S.A. Madrid, Spain
jaime.castaneda@itp.es

ABSTRACT

In order to investigate the unsteady flow behaviour in an HPT stage and the effects on the CFD solution of some numerical and physical modelling assumptions usually undertaken by the engineering community, an ITP in-house unsteady CFD code called Mu^2s^2T is first validated and then run under different configurations. The code is a fully unstructured code which solves the Reynolds averaged Navier-Stokes equations with a k-ω turbulence model. Hybrid meshes are used by having semi-structured meshes along the profile wall and fully unstructured triangular meshes on the inviscid region.

The VKI Brite Euram transonic turbine stage experimental test case is used for the investigation. This turbine is representative of a state of the art HPT and presents high potential interaction due to the vane shock waves. After validating the code in this case, the influence of typical engineering assumptions is investigated. First the influence of the rotor stagger angle is analysed, resulting in a high sensitivity of the predicted pressure level at the front part of the blade and a better matching with the experimental data when an opening of 1º is applied. The influence in the solution of applying an integer airfoil count ratio compared with the solution with exact number off computed by means of phase lagged boundary conditions is also investigated. Additional Euler and Navier-Stokes computations are presented and the influence of the viscous effects is discussed. Finally a simulation including vane trailing edge cooling is performed so that conclusions about the influence of the cooling can be drawn.

INTRODUCTION

The aerodynamic working environment of turbine airfoils is inherently unsteady, mainly due to the interaction with upstream and downstream blades. Vortical waves are generated by the action of the viscosity on the airfoil surfaces and are convected downstream along with the wakes and secondary flows. Pressure waves are generated by the airfoil loading and propagate in any direction. Both kind of perturbations can be found in turbines, but while in subsonic turbines the main source of unsteadyness is due to upstream vortical waves which generate unsteady pressure on the downstream airfoil surface and eventually unsteady boundary layer behaviour, in transonic airfoils the potential effects are much more important due to the higher Mach number conditions and eventually due to the presence of shock waves (Miller et al (2002)[9]). In all cases the unsteady perturbations on the airfoil surfaces generate pressure waves which propagates with different velocities upstream and downstream depending on the Mach number, generating the acoustic response of the system which itself depends on the interphase blade angle and reduced frequency. However in transonic cases the pressure perturbation due to the shock wave is one order of magnitude larger than the generated acoustic field and therefore the main contribution to the unsteady pressure on the rotor can be described by the events occurring during the stator/rotor characteristic passing time.

On the other hand, this pressure perturbations at the rotor blade can be very high, hence generating large unsteady forces on the blade, which can excite blade vibration and may cause High Cycle Fatigue (HCF) problems and therefore compromising the life. Therefore it is very important for turbine designers both to understand the origin of such unsteady forces and to develop the capability to accurately simulate them in order to be able to predict its effect on the blade vibration and eventually to be able to propose design changes to diminish such effects.

Thanks to faster computers and new numerical developments, unsteady CFD simulations tools are currently being used routinely by the turbomachinery industry to simulate quasi three dimensional (Q3D) unsteady flows due

to row interactions. While for describing the acoustics due to row interaction in subsonic airfoils it is possible to make use of linear methods, in transonic cases and due to the high non linearity associated to the shock waves, non linear methods are better suited for simulating the unsteady pressure interaction.
Although unsteady Navier-Stokes Q3D solvers have been extensively used by the turbomachinery community during the last years, it is still needed deeper validation with accurate and detail experimental data, together with further investigation on numerical and physical modelling effects in order to be able to asses the accuracy of the simulations and the relative importance of the different simplifications and assumptions.
The objective of the present investigation is to contribute to the physical understanding of the unsteady flow phenomena and to analyse the influence on the CFD simulation results of some simplifications and assumptions usually taken by the turbomachinery community. The test cases are based on the experiments performed at the von Karman Institute (VKI), on a transonic high pressure turbine (HPT) stage representative of the state of the art. The European turbomachinery community has extensively investigated these experiments. A basic insight into the experimental unsteady data as well as CFD simulations can be found in Dénos et al (2000)[3]. The case is been extensively used as a baseline case for unsteady CFD validation. Laumert et al (2000)[8] presented 3D unsteady simulations and Dénos et al(2000)[3] presented 2D unsteady simulations to help to the understanding of the flow phenomena. A contribution to the physical understanding of the unsteady phenomena on this case as well as a validation of the code used here are presented in Fernández-Castañeda and De la Calzada (2003)[6]. However it is still possible to further investigate the effects of simplifications and assumptions typically applied by the engineering community to these kind of simulations and this is the intention of the present investigation. In particular the effect of rotor restaggering, the effect of the viscosity, the effect of airfoil count ratio and the effect of vane trailing edge cooling flow are discussed in this investigation.

TURBINE STAGE TEST CASE

The transonic turbine stage investigated by VKI under the TATEF Brite Euram programme is used as test case for the CFD simulations. This configuration is a transonic HPT composed of 43 cylindrical vanes and 64 twisted blades. A view of the simulated geometry at mid span and the predicted Mach field is presented in Fig. 1. The flowpath is cylindrical on the stator and has a meridional divergence of 10% at the hub of the rotor. In the experiments a 3% of coolant flow is ejected through a vane trailing edge cut on the pressure side, however for this investigation a rounded vane trailing edge is used, as can be observed in Fig.1. Only for the investigation of cooling effects, a cut trailing edge geometry with coolant injection is simulated.
More Details of the geometry and operating conditions can be found in Dénos et al (2000)[3].

Fig.1. VKI stage configuration. Mach field

Main measurements data available includes inlet total pressure and temperature, inter stage pressures at hub and tip, stage exit total pressure and flow angle, and unsteady pressure at 24 positions around rotor mid section. Some other instrumentation is also included as described in Dénos and Paniagua (2002)[4], but they will not be used for comparison in this investigation.
For the computations presented here we have focused on the nominal conditions and mid span section. Total inlet pressure is 1.62 bars and total inlet temperature is 440 K. Inlet total to exit static pressure ratio is 3.06 giving a Reynolds for the rotor (based on chord) of 10^6 and an isentropic Mach number value of 1.03 at the stator exit. These conditions causes the stator to be choked generating a shock wave at the trailing edge.

CFD SOLVER

The code Mu^2s^2T (Multirow Unsteady Unstructured Specific Solver for Turbomachinery) solves the Reynolds-Average Navier-Stokes equations written in conservative form. The general solution scheme is based upon that of Jameson (see Jameson et al (1981)[7]). The convective terms are discretized using a cell-centered scheme based on the dual mesh. A blend of second and fourth order dissipation terms is added to capture shock waves and prevent the appearance of high frequency modes. Computation of viscous terms is based on the use of the Hessian matrix. Turbulence effects are taken into account by the two equations k-ω model, even though for the present investigation the y^+ distance to the wall is large and the viscous sub-layer may not be accurately simulated.

Nevertheless for the present investigation the turbulence effects are thought to play a minor role. An edge data structure is used to minimise memory access and increase the flexibility of the code to handle mixed elements. The integration in time is performed using an explicit fifth stage Runge-Kutta scheme, where the artificial viscosity terms are evaluated the first, third and fifth stages. Implicit residual smoothing may be used to increase stability limit of the scheme although this technique has not been employed in this work. Stream tube variation is taken into account for Q3D simulations. The sliding interface technique, which interpolates information across blade row interface, is used. Currently, only conservative variables are interpolated and therefore the flux conservation is not guaranteed. Phase-lagged boundary conditions allow to compute the exact airfoil count ratio while using just a configuration with 1 stator / 1 rotor. Two different implemented methods can be used to take into account the phase-shifted periodic boundary condition, the direct store of the raw signal (Erdos) or the Generalized Shape Correction (GSC) where only the Fourier coefficients of the raw signal are stored.

COMPUTATIONAL DETAILS

In order to investigate the origin of unsteady effects on the stage configuration, time accurate Q3D computations are run. This is performed by taking the mid section geometry of the stator with a rounded trailing edge (only for the investigation of cooling effect a cut trailing edge is used) and the rotor and by building an annular configuration corresponding to the mean radius providing a streamtube height variation equivalent to the total annulus height variation. Although some 3D effects may affect the solution at mid span (i.e. by modifying the effective streamtube height), Laumer et al (2000)[8] already performed 3D steady and unsteady computations and some main discrepancies with the mean time experimental data still remained unexplained. Additionally Dénos et al (2000)[3] already showed that good prediction of the unsteady behaviour could be achieved by Q3D simulation. The simulations presented here include the exact airfoil count of 43 vanes and 64 blades, and an approximate configuration with 2 vanes and 3 blades. In this last case, the rotor row was re-scaled by a factor 0.9923 whereas the stator row, which controls the mass flow rate, was left unaltered.

An in-house grid generation environment named G2D was used to generate the 2D mesh on the complete geometry. The mesh is comprised of an anisotropic quasi-structured mesh made of quads on the boundary layer and wake regions built by a semi-structured advancing normal method and a Delaunay triangulation with smoothing and node degree homogenisation in the rest of the domain (see Corral and Fernández-Castañeda (2001)[2]). In this case a finer grid is ensured on the stator surface and wakes since we are eventually interested in the accurate definition of the vorticity coming from the stator and convected downstream. In the rotor, the whole channel is equally refined to allow a homogeneous definition of the downstream waves propagation around the blades. First, a grid for one stator and one rotor is built for the cases of exact airfoil count computation and the generated mesh is repeated for the 2 stators and 3 rotors configuration.

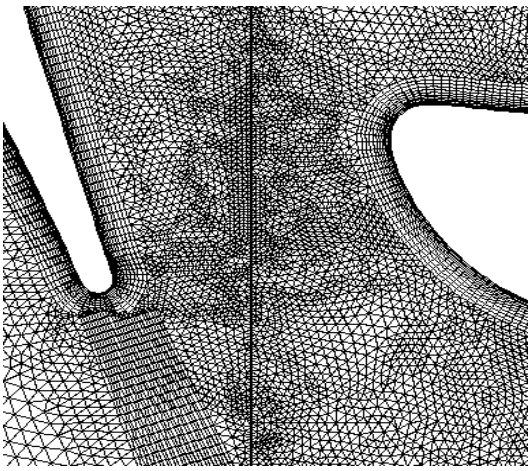

Fig.2. Hybrid mesh for viscous computation

Some details of a typical viscous grid on the nominal geometry can be observed in Fig.2. The general features of the 2 stators and 3 rotors configuration computations are summarised in Table 1. The unsteady convergence is based on the L^2 norm (see Burgos and Corral (2001)[1]). A simulation is considered converged when the unsteady norm has a value of 10^{-4}. An increase in the number of periods needed to converge the restaggered geometry is observed and attributed to the stronger shock pattern, which appears in this case. All computations were run in a Pentium IV 1.8 MHz. In the viscous calculations the physical time step used is 1.66×10^{-7}, which ensures a higher time resolution than the vortex shedding requires.

Simulation	No. Nodes	Iter./Period	Converg. Periods	CPU Time	CFL
Euler/Nom.Geom.	27963	1536	28	5 h.	3
Viscous/Nom. Geom.	58305	2592	26	22 h.	5
Viscous/Restagger.	58143	2304	86	66 h.	5

Table 1. Computation times

RESULTS AND DISCUSSIONS

Effect of Rotor Stagger Angle

One of the main unexplained differences between the experimental data and numerical simulations for this test case has been the shift in the time mean static pressure level obtained at the rotor forward part (see Fig. 3). Other computations performed on this configuration present such feature (see Dénos et al (2000)[3]). Including the stator cooling and/or the fully 3D geometry seems not to improve the solution (see Laumert (2000)[8]). Additionally the numerical results typically tend to underpredict the amplitude of unsteady pressure at the rotor crown.

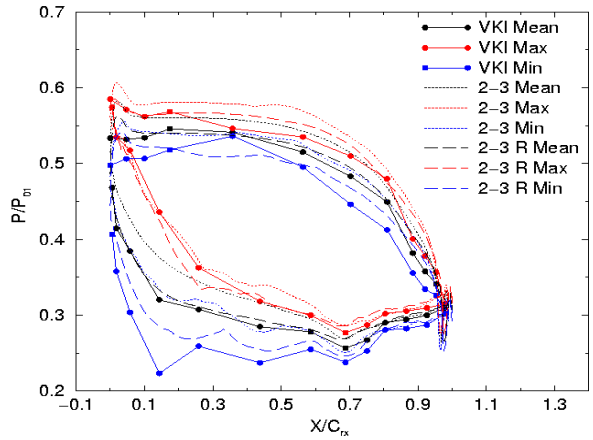

Fig.3. Rotor unsteady pressure envelope.
VKI: experimental data. Dotted line : simulations.
R : restaggered case

The mismatch between results is not only present at the suction surface, but also at the pressure surface while a good matching at the rotor aft surface is obtained (not surprising since the right static pressure at the exit is imposed in simulations). This seems to indicate that it is not a problem of local incidence but a problem of relative total pressure level. Since the stator is choked, mass flow can not be increased to overexpand the flow in the stator and the only additional parameters which can modify the stage reaction is the relative row exit flow angles. It is clear that vane exit flow angle can affect the interstage pressure level in HPT stages as shown experimentally by Dietrichs et al (1994)[5], however the aerodynamic performance of this stator alone has been already investigated extensively with good agreement between measurements and predictions (see Dunker (1993)[10]) and no uncertainty on the exit flow angle value is expected. On the other hand no measurements at the rotor exit have been performed on the rotating frame of reference and it is not very clear how the rotor relative exit flow angle could affect the stage reaction. In order to investigate the sensitivity of the results to the relative rotor exit angle, we made viscous computation with the rotor restaggered with an opening of 1º. The results, as can be observed in Fig. 3, show a large change in the static pressure levels at the rotor improving the matching with the experimental data and hence indicating their great sensitivity of these pressure levels to the rotor stagger angle. As can be seen in Fig. 4, where the velocity triangles of both configurations are represented, in the restaggered case the velocity at the stator exit is increased hence increasing the Mach number level and consequently generating a stronger shock wave. Additional results also showed an improvement: although the total to total pressure ratio increased from 2.72 to 2.73 compared with a measured value of 2.72, the exit swirl angle decreased from 22º to 17º improving respect to the measured value of 16º.

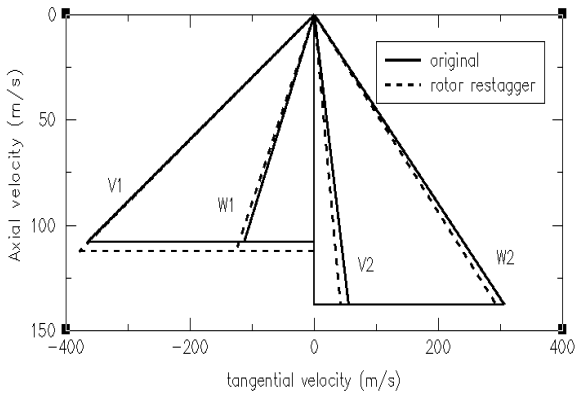

Fig.4. Stage velocity triangles

The unsteady pressure traces on the rotor are compared with experimental results in Fig. 5. The level of the maximum unsteady pressures obtained at the rotor accelerating region is now increased closer to the measured levels. However the double peak obtained in the experiments is lost in these new results compared with the original ones where an incipient double peak was present.

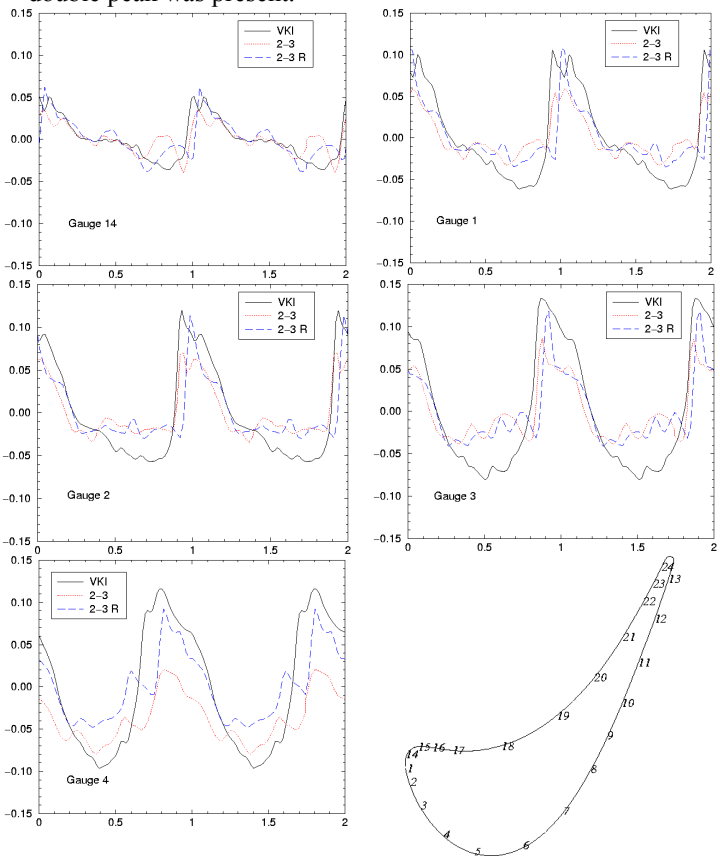

Fig. 5. $\Delta P/P_{01}$ unsteady pressure fluctuations at blade crown. Abscissa is phase in units of the stator's pitch-chord ratio. VKI: measurements. 2-3 nominal geometry. 2-3 R: computation with rotor restaggered

Effect of viscosity

The main goal of the inviscid calculation was to check whether the main source of unsteadyness in transonic cases can be predicted with the Euler equations, because such simulation may be more convenient due to the fact that the cost in CPU time of a Q3D simulation is five to ten times lower than a viscous one.

The unsteady pressure fluctuations obtained from the Euler simulation shows a similar pattern than the obtained in the viscous cases described in the previous section. This result was expected since the wake perturbation is one order of magnitude below the shock wave perturbation for this turbine stage configuration. Although not shown here, the pressure distribution on the vane shows that in the inviscid case a stronger trailing edge shock together with a stronger expansion wave in the rear part of the suction side is obtained, mainly due to the increase in the vane exit Mach number, while for the viscous case, the exit Mach reduces due to the increase in losses due to the boundary layer. The higher pressure perturbation produces larger pressure fluctuations on the rotor blade as can be observed in Fig. 6, where an improvement in the peak pressure is obtained compared with the viscous case. Note that due to the improvement in the strength of the expansion wave, the low pressure level of the perturbation is still reproduced, unlike the restaggered case (see Fig. 5) where although peak pressure was improved, low pressure perturbation level was worsen.

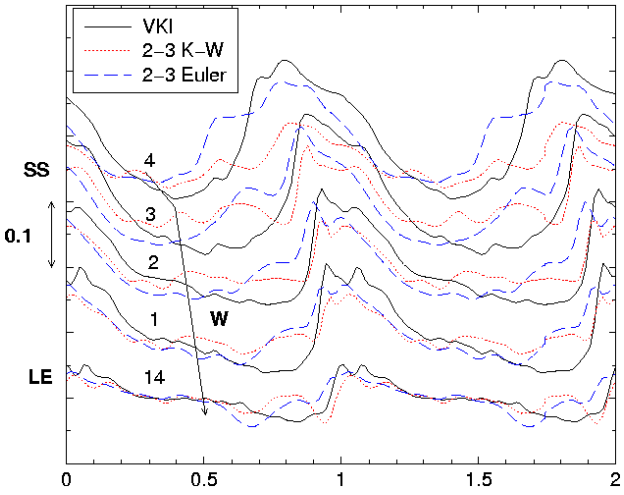

Fig. 6. $\Delta P/P_{01}$ unsteady pressure traces at rotor crown.

In a detailed analysis of the shape of the traces in the blade leading edge and crown region, some differences can be observed between de inviscid and the viscous computation (see Fig. 6. trace W). These differences may be attributed to the vane wake effect, however it is quite difficult to deduce such conclusion from the experimental results.

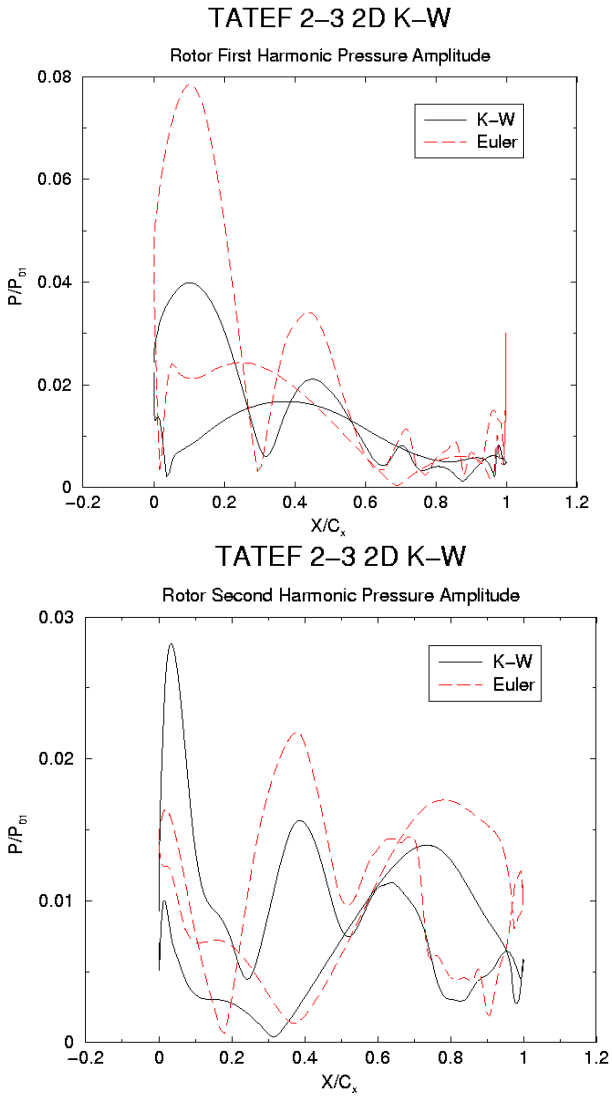

Fig. 7.First and second harmonics of unsteady pressure on viscous and inviscid cases (2/3 count ratio)

In order to better identify the differences between the viscous and inviscid results, comparison of first and second harmonic is presented in Fig.7. In the first harmonic both solutions are very similar except at the blade front suction side where the inviscid results presents higher pressure perturbation at the blade front suction surface. This could be expected since this perturbation can be identified as the main contribution of the shock wave when passing through the blade which is stronger in the inviscid case. It is probably more interesting to observe the second harmonic, in which the level of the unsteady pressure at the front part of the suction side is this time much higher in the viscous case, hence indicating that is the wake the main responsible of the second harmonic response in this area. However further downstream the shape of the perturbation is similar in both cases with the higher perturbation corresponding to

the inviscid case, hence indicating that is the pressure perturbation the main responsible of the response in this area. Moreover in the rear part of the blade pressure side the amplitude of the second harmonic of the unsteady pressure is higher than the amplitude of the first harmonic. This result is congruent with the obtained traces 19-24 showed in Fig. 8, where a double fluctuation over one period is present (traces D & E). Since this behaviour is observed in both computations the response of the rear part of the blade pressure can not be due to any viscous effect but must be due to the acoustic response of the perturbation produced by the shock wave. In fact, if the fourier transform of the potential perturbation is performed, it is observed that the harmonic content is quite wide with high levels up to 5^{th} harmonic. Although not shown here, it can be observed that the pressure response of the blade has similar levels of perturbation in harmonics 2^{nd} ,3^{rd} and 4^{th} .

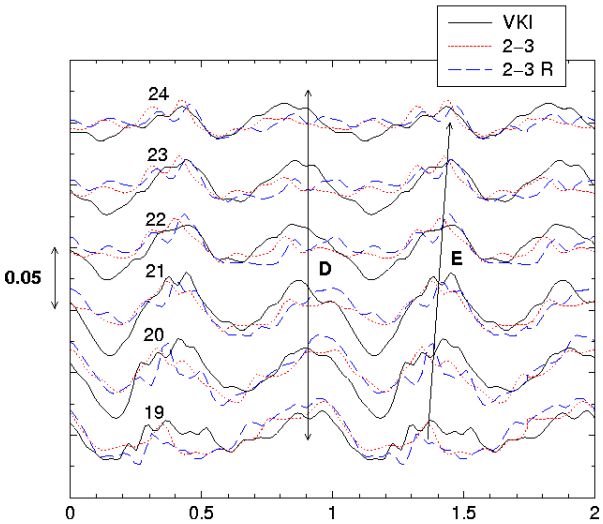

Fig. 8. $\Delta P/P_{01}$ Unsteady pressure traces on the aft pressure side region of the blade, with two events (D & E) per period

Effect of airfoil count ratio

Four representative cases have been simulated, one with the exact count ratio (43/64), and another with a reduced number (2/3), in inviscid and viscous modes. The pressure envelopes of the 4 cases can be seen in Fig. 9. The most remarkable difference is that in viscous cases it seems that due to the weakening of the shock no effect of the count ratio is observed, while in inviscid cases, where the effect of the shock is stronger, the exact case has about 20% higher unsteady perturbation level which tends to improve the prediction compared with the experimental data. Differences are present in all harmonics which are typically increased in 10% in the exact count case, while no differences are found in the harmonics of the viscous case.

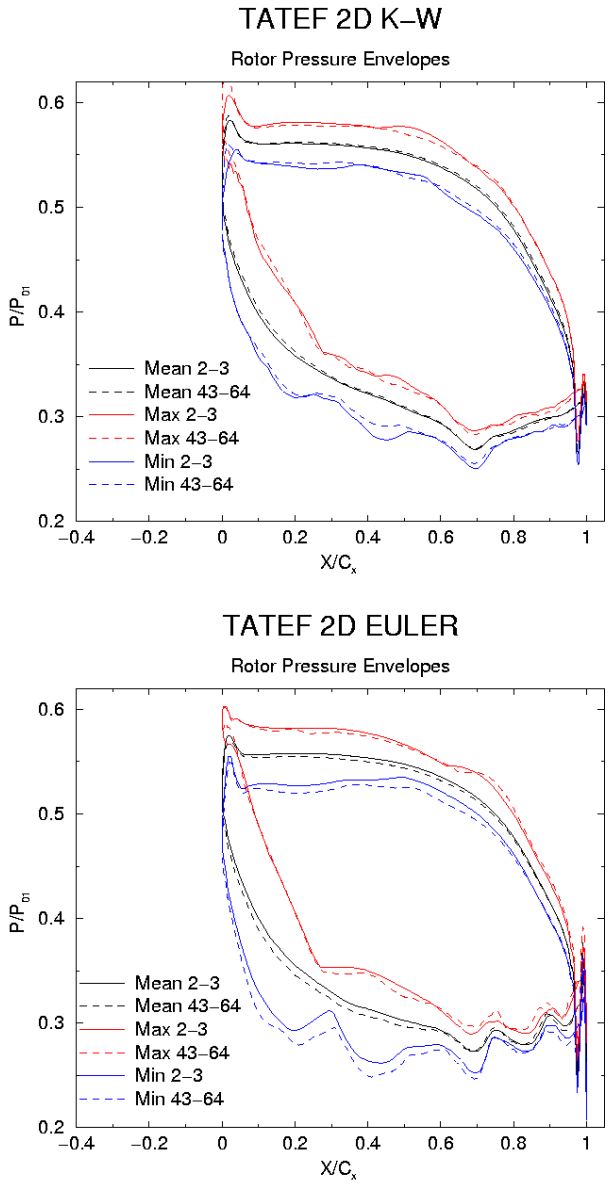

Fig. 9. Pressure envelopes for viscous (a) and inviscid (b) cases for 2/3 and 43/64 count ratio numbers

Effect of trailing edge cooling

Finally a viscous case including the trailing edge slot and 3% of cooling is included. In this case the local trailing edge cut present in the hardware used for the experiments is reproduced in the simulations (see Fig. 10). The results of unsteady pressure envelopes at the vane and blade is presented in Figs. 11 and 12. As previously reported in Dunker (1993)[10] about the experiments, the trailing edge cut reduces the effective trailing edge blockage and also modifies locally the effective geometry seen by the the main flow at the trailing edge pressure side, hence avoiding the corresponding shock wave to appear as is clearly can be seen in the pressure distribution at the vane, where no shock

at the throat appears. However it has to be pointed out that the trailing edge suction side a weak shock wave is still present.

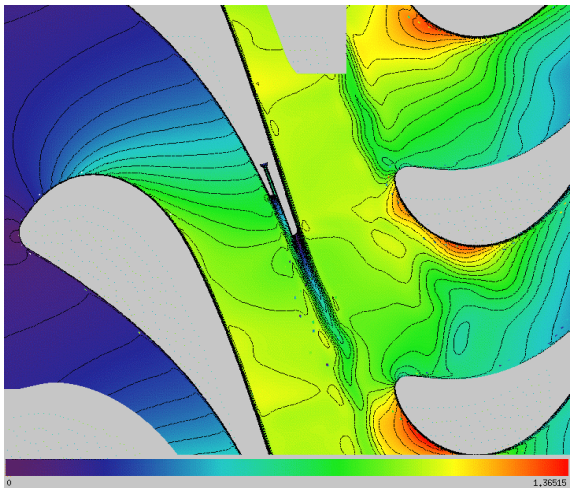

Fig.10. Vane trailing edge cooling. Absolute Mach number field and isloines

The influence of the cooling has two effects on the blade: one is reducing the level of the unsteady response at the suction side, and the other one is increasing the time mean value. Both effects are thought to be due to a increase in the vane exit pressure level which reduces the relative total pressure at the blade inlet, modifying the static pressure level reached at the blade surface (similarly to the restaggered case) and which also reduces shock wave strength and the associate perturbation.

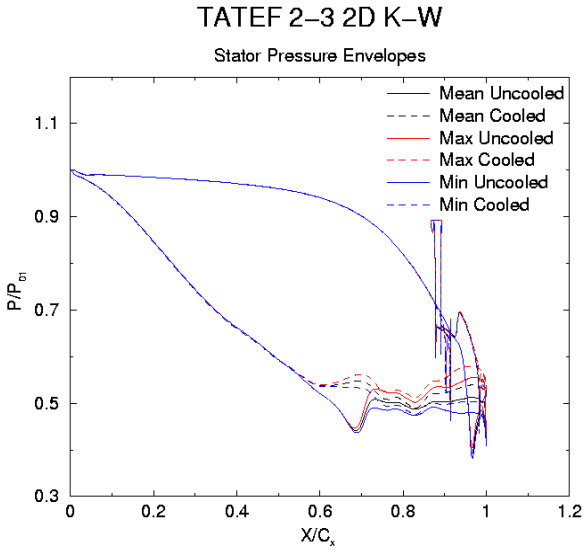

Fig. 11. Unsteady pressure envelopes on the vane surface

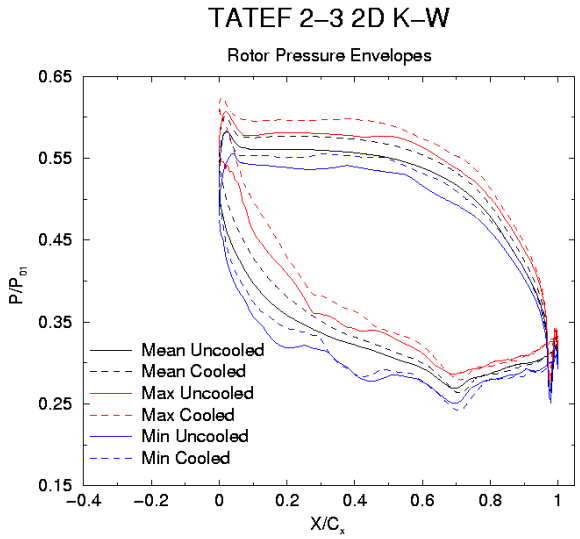

Fig. 12. Unsteady pressure envelopes on the rotor surface

CONCLUSIONS

The capability of an in-house non-linear CFD unsteady code (Mu^2s^2T) to simulate unsteady aerodynamic interaction effects in turbines has been shown by computing the VKI Brite Euram transonic stage. The case has been run by a turbulent Navier-Stokes Q3D 2 stator / 3 rotor computation reproducing the mid span section of the experiment. Since a shift in the predicted time mean static pressure on the rotor was obtained compared to the measurements, the possible source for such a difference was investigated. A case was computed with a rotor restaggering of 1º open in order to investigate the sensitivity to this parameter and results were shown to improve due to the change in the interstage pressure. The stator shock wave strength is observed to increase, hence increasing the maximum level of the unsteady pressure on the rotor crown, getting closer to the measured values. Additionally the absolute exit swirl predicted reduced getting closer to the measured value. Therefore the differences observed in pressure level at the rotor surface between the simulations on the original geometry and the experiments could be explained by a difference on the predicted rotor relative exit flow angle.

The predicted and measured unsteady pressure on the rotor surface has been compared with the measurement data and explanation to the different unsteady phenomena has been given, showing the main source of the observed perturbations. The shock wave coming from the stator trailing edge was identified to impinge at the rotor crown and then to sweep to the leading edge creating the larger pressure perturbation. Additional shock wave reflections along the channel generates new pressure waves which define the pressure response further downstream.

In order to investigate if any of the effects on the rotor can be identified to be due to the wake, Euler computations

were performed and the results were compared with the turbulent viscous solution. Wake effects were only identified to be important at leading edge accelerating region were a clear maximum in the amplitude of the second harmonic appeared, being also identifiable at the unsteady pressure traces. Therefore it is concluded that for this configuration inviscid simulations are accurate enough for predicting main unsteady forces on the rotor, and furthermore the amplitude of the unsteady response on a significant part of the rotor surface is also better predicted by the inviscid simulation.
The effect of the exact count ratio compared with a reduced integer number is performed by running a 1/1 ratio applying phase lagged boundary conditions. Exact count ratio can increase the level of the unsteady pressure on the rotor up to 20% when running inviscid cases compared with the 2/3 case. Therefore it is recommended to run the exact count ratio when performing such computations. However no sensitiveness to these count ratios is observed when running viscous cases, hence indicating that viscosity can have an effect large enough to mask some other modelling simplifications as the count ratio.
Finally the effect of the vane trailing edge cooling flow on the rotor unsteady pressure is investigated, showing that the main effect of the cooling is to reduce the vane pressure ratio, hence reducing the shock strength and the corresponding response on the rotor. Additionally the cooling increases the stage reaction therefore increasing the time mean pressure level at the rotor suction side.

ACKNOWLEDGMENTS
The above research is based upon work funded by the Commission of the European Communities as part of the Brite Euram "Turbine Aero-Thermal External Flows (TATEF)" under contract BRPR-CT97-0519. The authors wish to acknowledge the support from VKI – von Karman Institute for Fluid Dynamics.

REFERENCES

[1] Burgos, M. A., Corral, R., (2001), *Application of Phase-Lagged Boundary Conditions to Rotor/Stator Interaction*, ASME paper GT-2001-586.

[2] Corral, R., Fernández-Castañeda, J., (2001), *Surface Mesh Generation by Means of Steiner Triangulations*, AIAA Journal Vol. 39, No. 1, pp. 176-180.

[3] Dénos, R., Art, T., Paniagua, G., Michelassi, V., Martelli, F., (2000), *Investigation of the Unsteady Rotor Aerodynamics in a Transonic Turbine Stage*, ASME paper GT-2000-435, Journal of Turbomachinery, Vol. 123, pp 81-89.

[4] Dénos, R., Paniagua, G., (2002), *Influence of the Hub Endwall Cavity flow on the Time-Averaged and Time-Resolved Aero-Thermodynamics of an Axial HP Turbine Stage*, ASME paper GT-2002-30185.

[5] Dietrichs,H.J., Malzacher, F., Broichausen, K., (1994), *Development of a HP-Turbine for a Small Helicopter Engine*, paper 27 on AGARD Conference Proceeding 537 "Technology Requirements for Small Gas Turbines".

[6] Fernández-Castañeda, J., De la Calzada, P. (2003) "*Numerical Simulation of Unsteady Flow in an HPT stage*". European Turbomachinery Conference, April, 2003, Prague, Checoslovaquia.

[7] Jameson, A., Schmidt, W., and Turkel, E., (1981), *Numerical Solution of the Euler Equations by Finite Volume Techniques Using Runge-Kutta Time Stepping Schemes*, AIAA paper 81-1259.

[8] Laumert, B., Martensson, H., Fransson, T., (2000), *Investigation of the Flowfield in the Transonic VKI Brite Euram Turbine Stage with 3D Steady and Unsteady N-S Computations*, ASME paper GT-2000-433.

[9] Miller, R.J., Moss, R.W., Ainsworth, R.W., Harvey, N.W., (2002), Wake, shock and Potential Field Interactions in a 1.5 Stage Turbine: Part 1: Vane and Rotor-Vane Interacton, ASME paper GT-2002-30435.

[10] Several Authors, Edited by Dunker, R., DGXII, European Commision, (1993), *Advances in Engine Technology*, European Commision Aeronautics Research Series.